EVALUATION OF LIQUEFYING SOIL THROUGH TIME USING SYSTEM IDENTIFICATION

Steven Glaser, Division of Engineering, Colorado School of Mines
Riley Chung, Structures Division, National institute of Standards and Technology

ABSTRACT

A new approach to evaluating earthquake strong motion, parametric modeling (System Identification) is introduced. This method avoids many of the problems inherent in Fourier Methods. Both stationary and recursive parametric modeling methods are applied to input-output data sets from the Wildlife Site, CA, which was subjected to two large earthquakes on November 24, 1987. During the second, larger, earthquake (Superstition Hills earthquake) the site soils liquefied. The data set collected is unique since it is the only available record of buried and surface motions publicly available. Existing seismological analyses of the two earthquakes show that the Superstition Hills earthquake actually consisted of three distinct subevents. The strong motion records and pore water pressure records show excellent correlation with the subevents. The results show weakening of the soils system as pore pressure increases, with estimates of natural frequency, damping ratio, and participation factor given.

INTRODUCTION

The traditional method of geotechnical analysis of dynamic soil motions in earthquake engineering is by the Fourier transform. However, serious problems arise when this method is applied to short data streams, and to signals changing through time — non-stationary signals. These and other serious limitations of the Fourier method are examined in detail in many books and journals (e.g., Glaser, 1993; Johansson, 1993; Pandit, 1991). This study was undertaken to show the effectiveness of a different type of model, a parametric mode commonly used in automatic control and geophysics. An important aspect of the parametric models used, is that there is a theoretical link between the system parameters and the damping and stiffness on an N-Degree-of-Freedom System. This method requires (as do all inverse methods!) a time history if the signal input into the system, and a corresponding system output. The method allows estimates of a system's dynamic properties to be to be made if an input-output data set is available.

An obvious application of this method, commonly referred to as system identification (SI), is to estimate the dynamic soil properties of a profile excited by earthquake strong motion. This would yield large strain soil properties, and avoid sampling disturbance. The records of the two (Elmore Ranch and Superstition Hills) 1987 earthquakes at the Wildlife Site in the Imperial Valley, California are the only publicly available true input-output data sets.

This paper applies several parametric models to the input-output data set recorded during the 1987 Superstition Hills earthquake. Since the inverse problem is non-unique, it is necessary to understand the mechanistic behavior of the system being modeled in order to select the correct model and solution. To this end detailed geotechnical, geological, and seismological analyses of the Wildlife site and earthquake events are presented

SYSTEM IDENTIFICATION

Parametric Modeling of the Soil System

The goal of system identification is to model a system in a manner that provides needed mechanical information about that system. The system is often visualized as a filter with a known input and output. In the time domain, the linear filtering process of a signal passing through a soil layer is represented as a convolution. The process of inversion, or deconvolution, allows the estimation of the system response function (filter) if the input and output signals are known. A simple model for characterizing a system is as a ratio of weighted polynomials. The weights are the parameters relating system input and output. Such a model, referred to as an autoregressive-moving average (ARMA) model, is based on discrete time series analysis:

$$y_t = b_0 x_t + b_1 x_{t-1} + \ldots + a_1 y_{t-1} + a_2 y_{t-2} + \ldots \quad (1)$$

where y_j is the actual output data sequence, x_j is the input sequence (assume white noise for simple spectral estimation), and t is the time step counter. Equation 1 is often rearranged to give

$$y_t = a_1 y_{t-1} + a_2 y_{t-2} + \ldots + b_0 x_t + b_1 x_{t-1} + \ldots \equiv \left(\sum_{j=0}^{nb} b_j x_{t-j} + \sum_{k=1}^{na} a_k y_{t-k} \right) \qquad (2)$$

where *na* and *nb* are the AR and MA orders, respectively. The output is seen as a combination of the input history acted upon by the "*b*" coefficients plus the past outputs acted upon by the "*a*" coefficients. The input series, involving the "*b*" coefficients, is a causal moving average (MA) process (convolutional). The series involving weighted past output values ("*a*" coefficients) is a noncausal autoregressive (AR) process. The lengths of the AR and MA processes (model order) must be explicitly chosen so that the model best represents the process.

Applying the shifting theorem to Eq. 2. yields the Fourier transform (Bracewell, 1978)

$$Y_\omega \left(1 + a_1 e^{i\omega} + a_2 e^{2i\omega} + \ldots \right) = X_\omega \left(b_0 + b_1 e^{i\omega} + b_2 e^{2i\omega} + \ldots \right) \qquad (3)$$

where i is $\sqrt{-1}$ and ω is circular frequency. Applying the Z-transform (Bracewell, 1978), where $z^k = e^{ki\omega}$, and rearranging, yields the frequency domain transfer function H_ω

$$H_\omega = \frac{Y_\omega}{X_\omega} = \frac{b_o + b_1 z^1 + b_2 z^2 + \ldots}{1 - a_1 z^1 - a_2 z^2 + \ldots} \qquad (4)$$

The ARMA model is very powerful in that it can easily model sharp drops, sharp peaks, and smooth spectral behavior. It is also the most parsimonious estimator (Robinson, 1982), describing a complex process with very few parameters calculated from a small length of data, avoiding many of the difficulties inherent in the traditional Fourier methods.

The ARMA model has special significance since it can be derived directly from the differential equation of motion for an *N*-degree-of-freedom system, with the damping ratio and resonant frequency as the model parameters (e.g., Gersch and Luo, 1970). A $2n$-$2n$ ARMA model is therefore a valid model for a layered soil system, or soil-structure interaction problem. The damping ratio and resonant frequency of the *N*-degree-of-freedom oscillators are contained in the $2n$ AR parameters. Phase relations are preserved in the MA parameters. Extensions of this model, e.g., ARMAX, ARX, Box-Jenkins, allow input, system, and output noise to be expressly modeled (Ljung, 1987). In particular, the ARX model includes the effect of uncertainties and noise as a white noise term. The structure is written as

$$A_i y_t = B_j x_{t-k} + e_t \qquad (5)$$

where k is a time step delay and e_t is a white noise sequence.

Stationarity

Traditional methods of system estimation, both parametric and non-parametric, are strictly valid only for stationary data. A stationary signal is one whose statistics do not change with time. The commonly invoked, loose definition of stationarity requires that the signal variance be constant over any and all time windows. Inherent in a stationary transformation is the averaging of the signal components over the sampling period T. The energies present at each component frequency are integrated over the entire time period T. The difficulty with non-stationary signals is that these energies are changing during this period. If the frequencies present are changing over this time window, the resulting estimation, regardless of method used, will be a smeared average as if all the frequencies with energy were active throughout the period.

The field of adaptive (recursive) filtering was developed to model non-stationary processes. As the statistics of the signal change through time, the filter "adapts" to the changing variance with new parameter values that reflect the structure of the system at that point. The predicted value for the next time step can be compared with the actual value, and the difference will give a measure of how well the filter is doing its job. ARMA or AR parameters can be sequentially estimated so that the parameters are adaptive to the changing nature of the process (Ljung, 1987). The parameters are updated after each data point, tracking slowly non-stationary signals. The spectral estimation can be made at any time step by evaluating the AR parameters around the unit circle, giving the spectral description of the behavior of the process at that time. The most popular direct adaptive filter, or process model, is the Kalman filter (Kalman, 1960). Sorenson (1970) points out that the Kalman approach is a direct descendant of Gauss's least squares, except now neither the signal nor the noise model is stationary — the state may change from sample point to sample point. The so-called extended Kalman filter has been very successfully applied to non-linear estimation problems

THE WILDLIFE SITE IN THE IMPERIAL VALLEY

Introduction

The Wildlife site is located in the Western Imperial Valley, 13 km north of Brawley, Imperial County, California. The Imperial Valley is one of the most seismically active regions of the United States (Hudnut and Sieh, 1989). The Wildlife site is located in the Imperial Wildlife Management Area, on an incised flood plain of the Alamo river (Bennett et al., 1984). The deposits consist of various flood plain, fluvial, and lacustrine materials with 7 distinct units in the first 26 m. The top three units were investigated thoroughly since they were believed to be the seat of any liquefaction (Holzer et al., 1989).

The geotechnical cross-section of the first 13 m of soil at the Wildlife is shown in Fig. 1. The water table, controlled by the near-by Alamo river, was approximately 1.2 m below the surface when the Superstition Hills earthquakes struck. Unit A is a very soft sandy to clayey silt, which grades into the silty clay of at the bottom of Unit B below. The upper meter of Unit B, B1, is a very loose poorly graded silty sand which phases towards the denser silty sand of subunit B2. In general, the materials in Unit B grade from coarsest at the bottom (7 m) to the finest at the top. Unit C ranges

from a medium-to-stiff clayey silt to a very stiff silty clay. Unit D is a dense, well-graded silt, cemented towards the top of the unit.

The U.S. Geological Survey (USGS) chose to install an instrumentation array at the Wildlife site because it liquefied during the 1981 Westmoreland earthquake (shear magnitude, M_S, 6.0) and its location in a very seismically active area. Besides surface and buried (8 m) accelerometers, an array of pore pressure transducers was installed at various depths, making this one of four piezometric arrays in the U.S. (Holzer et al., 1989; Brady et al., 1989). Fig. 1 presents the physical relation of the piezometers to the soil units. Two piezometers were installed in subunit B1, three in B2, and one in the dense clayey silt of Unit D.

The USGS undertook a thorough site investigation at the time the instrumentation array was installed (Bennett et al., 1984), and other researchers performed geophysical investigations to determine the in situ shear-wave velocity (Bierschwale, 1984; Nazarian and Stokoe, 1984). Both standard penetration tests and cone penetration tests, as well as an analysis of the soil description, indicated that subunit B1 would be the most likely to liquefy in the event of strong enough dynamic excitation. Piezometer P5 and P2 were installed in this subunit.

Two large earthquakes, the Elmore Ranch and Superstition Hills, occurred on November 24, 1987. The shaking was strong enough to induce liquefaction at the Wildlife site, which suffered more than 2 m of lateral spread towards the Alamo river, and sand boils occurred over at least 33 hectares (Holzer et al., 1989). Accelerograms from the buried and surface transducers, as well as pore pressure histories, were captured for both the Elmore Ranch and Superstition Hills earthquakes (Brady et al., 1989). This is the only full input-output data set known to exist for a site experiencing liquefaction, and the only set of records complete enough to allow an unambiguous system identification analysis.

Geology

The Imperial Valley is a structural depression caused by the active spreading of the Gulf of California (Magistrale et al., 1989). The Wildlife site is located 32 km west of the Superstition Hills temblor epicenter. The Valley flanks are continental crystalline plutonic and metamorphic rocks, about 2 km deep on the west, while the center of the central Valley is comprised of metamorphosed sedimentary rocks beneath 5 km of sediment (Magistrale et al., 1989).

The surface sediments in the areas of interest are Holocene lacustrine silty sand and claystone, interbedded with alluvial deposits, below which are slightly consolidated Pleistocene silty and clayey lake deposits with sand and gravelly units (Bennett et al., 1984). The impedance contrasts of the geology are such that the vertical motions due to a local earthquake are primary-waves (P-waves), while the horizontal motions are manifestations of the passage of shear-waves (S-waves) (Wald et al., 1990). This assertion is borne out by the phase shift that occurred between the buried and surface horizontal motion records and by the lack of shift in the vertical records.

The Superstition Hills fault is a northwest-trending fault that can be seen as a continuation of the San Andreas and San Jacinto fault zones. Evidence shows that the Superstition Hills fault delineates a section of the boundary between the steeply sloping crystalline basement and the sedimentary materials, with a great amount of historical northwest-trending tectonic activity in the region (Magistrale et al., 1989).

Seismology

On the evening of November 23, 1987, an earthquake occurred along the previously unknown Elmore Ranch fault, with an M_S of 6.2 and a hypocenter depth of about 11 km (Magistrale et al., 1989). The fault was a north-east trending, left-lateral displacement made up of a multitude of small displacements or fault zones. The maximum measured surface horizontal displacement was 125 mm, which occurred during the event itself. Twelve hours after the Elmore Ranch earthquake, a larger, long-duration earthquake struck on the Superstition Hills fault. This 6.6 M_S seismic event was caused by a northwestward-striking right lateral displacement coincident with previous earthquakes in 1968 and 1979 (Magistrale, 1989). The two 1987 temblors, Elmore Ranch and Superstition Hills, are associated with a well-defined conjugate fault system (Hudnut et al., 1989). The left-lateral motion relieved normal stress on the existent major northwest-striking fault system, allowing the shear stress from the Pacific plate to be relieved.

The Superstition earthquake was a complicated event characterized by an extended period of strong motion (Wald et al., 1990). Figure 2 shows the acceleration record for the north-south acceleration, recorded at a depth of 8 meters. There appears to be arrivals of energy at approximately 3 and 9 seconds following the arrival of the initial S-wave. Thorough and independent study of the strong motion and teleseismic records by several researchers indicates the event was made up of three distinct subevents that had to have occurred over an extended area (Hwang et al., 1990; Wald et al., 1990; Frankel and Wennerberg, 1989) The physical location of these subevents is given in Fig. 3 in both the map and plan view. While all three studies reached essentially the same general conclusions, the study by Wald et al. was the most exhaustive and their quantitative results will be used in this paper.

Wald et al. (1990) calculated the arrival times relative to initial energy arrival, seismic magnitude, and horizontal extent of the three subevents. While the M_S of the three subevents are very similar, the energy released by subevent 3, characterized by the seismic moment, is almost 3 times larger than the combined energy release of the first two subevents. The source durations of the first two subevents were short (less than 2 s for subevent 2), while it was estimated that subevent 3 required about 7.5 s for the displacement to propagate the 18 km (Wald et al., 1990). The calculated arrival times of the three subevents are shown in Fig. 2, exactly matching the visually perceived arrival of packets of energy. The extended shaking due to subevent 3 continued for slightly longer than the 7.5 s duration of source displacement. While the propagation velocity of each subevent was greater or equal to the S-wave velocity, the very slow rupture velocity for the entire earthquake implies an overall rupture mechanism reminiscent of progressive failure (Frankel and Wennerberg, 1989).

Pore Pressure History

Analysis of pore pressure histories recorded during the Elmore Ranch and Superstition Hills earthquakes yields additional understanding of the mechanistic behavior of the Wildlife site. Complete pore pressure records were made during both temblors at five different depths (Brady et al., 1989). Records show that an increase in pore water pressure was measured during both the Elmore Ranch and Superstition Hills earthquakes.

This paper will focus on the pore water pressure history of piezometer P5, which was buried at a depth of 2.9 m, the top of soil layer B1. This transducer is being singled out for several reasons: it unambiguously indicated that the excess pore pressure exceeded the total overburden pressure; it was located at the top of the layer expected to liquefy during the Superstition Hills shaking and therefore would be at the point of initial liquefaction (Scott, 1987; Florin and Ivanov, 1962).

Figure 4 introduces the pore pressure ratio r_u (ratio of excess pore pressure u to initial effective overburden stress $\bar{\sigma}_v$) history for piezometer P5, Superstition Hills earthquake, compared to the acceleration record of Fig. 2 (Brady et al., 1989). The pore pressure history is addressed here to enhance mechanistic understanding of the recorded strong motion signals and thus simplify and strengthen later interpretation. There is some controversy whether the pore pressure transducers at the site were operating properly (Hushmand et al., 1992, 1991), however, it was decided to utilize what clues the data provides without making a value judgement.

At time t_0 (Fig. 4) the initial S-wave energy from the first subevent arrived, and a very slight increase in pore pressure was recorded by P5. At approximately time $t_{3.1}$ (subscript is elapsed time) energy from subevent 2 excited the accelerometer, and the pore pressure started to increase at a steady rate. Finally, at time $t_{9.8}$ strong shaking was triggered by the arrival of subevent 3, and the pore pressure ratio at P5 increased at a rapid rate to a maximum greater than 1.2. After $t_{9.8}$ the rate of increase of r_u was relatively constant for the duration of source motion (≈7.5 s), until it reached 0.6, a level often considered as functional liquefaction. The rate of pore pressure increase slowed until approximately time t_{23}, at which time r_u was approximately 1 and the rate of increase remains nearly constant. This strong correlation between pore pressure and seismic history indicates more than serendipity.

IDENTIFICATION OF THE WILDLIFE SITE SOIL SYSTEM

Analysis Methods

For the problem at hand, estimating the soil parameters during the Superstition Hills earthquake at the Wildlife site, both the system input and output are known. Analysis of the records was undertaken using the standard routines contained in the MATLAB System Identification Toolbox (MathWorks, 1991). Since there is little known about the statistics of the system, a direct method was used to determine whether a given model accurately captured the system — the output simulated by the calculated system had to accurately model the actual measured output.

The input-output data record was initially broken into segments based on the mechanistic understanding discussed in previous sections. Segment 1 is the segment from the start of the time history to the arrival of subevent 2 at approximately $t_{2.8}$ seconds (171 data points). Segment 2 runs from the arrival of subevent 2 to the arrival of subevent 3 at approximately $t_{8.8}$ seconds (150 data points). The segment corresponding to the shaking due to subevent 3 is assumed to be very non-stationary due to the nature of the signal and the rapid rise of pore pressure. Segment 3 encompassed the coda of the signal after the shaking stopped at approximately t_{17} seconds, to the end of the record at 93 seconds (1870 data points). If the stationary model could not accurately and parsimoniously simulate the segment output, a non-stationary recursive model was used. In addition, the residual autocorrelation function, and the cross-correlation function between the input and output residuals were white with 99 percent confidence (Bohlin, 1987). A final verification on independent input-output data was made using the 90° Superstition Hills record, and the Elmore Ranch time histories.

Once the relevant model is determined and the parameters calculated, a spectral representation of the system is easily obtained from Eqn. 4. The statistical approach used in parametric modeling allows the calculation of confidence intervals of the spectral estimate. The modal natural frequencies ξ_j, percent of critical damping ω_j, (Ghanem et al., 1991) and power participation factor p_j (Pandit, 1991; Safak, 1988) are calculated from the system poles and residues found from partial-fraction expansion of Eq. 2.

Results

The first two segments, corresponding to the beginning of the record up to the arrival of subevent 3, can be accurately modeled by stationary ARX models. Segment 1 is modeled as a 4-DOF system, with an RMS error between simulated and actual velocity of 0.26. Segment 2 proved to be representable as a 3-DOF system, with an RMS error between simulated and actual velocity of 1.1. A comparison of the spectral estimates is shown in Fig. 5, along with the estimates of modal parameters. These values are summarized in the top of Table 1. Note that the system natural frequency diminished slightly after the arrival of subevent 2, an indication of system softening.

The change in the soil system was so slight during the initial 8.8 s of excitation, that it proved possible to model a combined initial segment (subevents 1 and 2) accurately with one 4-DOF ARX model (RMS error = 0.59), with the characteristics of the second subevent swamping the lower energy first arrival. The suitability of this model is verified by comparing the actual surface velocities from the Elmore Ranch 360° horizontal record with the record simulated for the relevant Elmore Ranch input by the selected model. The congruity between simulation and real-life is shown in Fig. 6, which match with an RMS error of only 0.72.

In order to see the evolution of the soil system through the initial 20 s of the Superstition Hills earthquake, the system was modeled with a recursive technique employing a Kalman filter model with 3-DOF. The spectral time history of the top 8 m of the Wildlife site for the initial 20 s of shaking is shown in Fig.7. The softening corresponds with the initial increase in pore water

pressure to about 3.1 kPa, accounting for the downward shift in natural frequencies and increase in damping.

The system behavior during the subevent 3 strong shaking is obviously non-stationary and non-linear due to the rapid build-up of pore water pressure and irregular shaking. The point at which a stationary model could no longer model the system behavior corresponds to the time when the pore pressure ratio reached approximately 0.6, at $t_{16.5}$. The modal estimates from a Kalman filter model showed that the natural frequency diminished and damping ratio increased as the effective stress in soil layer B decreased, and are summarized in the bottom of Table 1.

The final segment (post-energy input) proved to be quite non-stationary due to the constant increase in phase shift between buried and surface signals, and it was not possible to accurately model the soil as a time invariant system. Application of a 3-DOF, 0 delay Kalman filter captures the essence of the soil response through time (RMS error = 0.76), with the spectral time history shown in Fig. 8. As indicated by the time dependent values for resonant frequency and damping, the soil system is slowly changing as the pore water pressure comes to equilibrium.

CONCLUSIONS

The Wildlife Site, CA was subjected to two large earthquakes on November 24, 1987. During the second, larger, earthquake (Superstition Hills earthquake) the site liquefied. The data collected are unique since they are the only available records of buried and surface motions publicly available. In addition, pore water pressure records were recorded at several depths during the temblor.

The Superstition Hills earthquake was actually three distinct subevents. The third subevent was the largest, associated with displacement along 18 km of fault. The strong motion records and pore water pressure records were examined, and showed excellent correlation with the subevents. A significant rise in pore pressure that resulted in liquefaction of layer B occurred at the onset of subevent 3.

Both stationary and recursive parametric modeling methods are applied to the unique input-output data set from the two temblors. These unique results show weakening of the soils system as pore pressure increased. A summary of the calculated dynamic system properties is given in Table 1. The parametric models used in this study are powerful tools for the qualitative and quantitative estimation of in situ soil properties. The recursive methods allow the behavior of the soil system to be monitored throughout the excitation process and liquefaction. Figures 7 and 8 present a unique insight into the liquefaction process The confidence in the estimates is increased by comparison with independent data from the E-W direction, and the Elmore Ranch temblor. The estimates all converged on the values reported. The soil was 'tested' in its natural condition, with no man-made disturbances or other difficulties encountered in the laboratory.

BIBLIOGRAPHY

Bennett, M. J., McLaughlin, P. V., Sarmiento, J. S., & Youd, T. L. (1984). *Geotechnical investigation of liquefaction sites, Imperial Valley, California,* Open File Report 84-252. p. 103. Menlo Park, CA: United States Geological Survey.

Bierschwale, J. G. (1984). Analytical evaluation of liquefaction potential of sands subjected to the 1981 Westmoreland earthquake. *University of Texas geotechnical engineering report GR-84-15. p.* 231. Austin TX: University of Texas Geotechnical Engineering Center.

Bohlin, T. (1987). Model validation. *Encyclopedia of systems and control* (Singh, M.) Oxford: Pergamon Press.

Bracewell, R. N. (1978). *The Fourier transform and its applications.* p. 443 New York: McGraw-Hill.

Brady, A G , Mork, P. N., Seekins, L C., & Switzer, L. C. (1989). *Processed strong-motion records from the Imperial Wildlife liquefaction array, Imperial County, California, recorded during the Superstition Hills earthquakes, November 24, 1987.* Open File Report 97-87. p. 115. Menlo Park, CA: United States Geological Survey.

Florin, V. A., & Ivanov, P L. (1961). Liquefaction of saturated sandy soils. *Proceedings of the fifth international conference on soil mechanics and foundation engineering. I* Paris. 107-111. Paris: Dunod.

Frankel, A., & Wennerberg, L. (1989). Rupture Process of the MS 6.6 Superstition Hills, California, earthquake determined from strong-motion recordings: application of tomographic source inversion. *Bulletin of the Seismological Society of America,* 79(2), 515-541.

Gersch, W., & Luo, S. (1972). Discrete time series synthesis of randomly excited structural system response. *Journal of the acoustic society of America, 51*(1), 402-408.

Ghanem, R. G., Gavin, H., & Shinozuka, M. (1991) *Experimental Verification of a number of structural system identification algorithms.* p. 302. Technical Report NCEER-91-0024. Buffalo: National Center for Earthquake Engineering Research.

Glaser, S. (1993). *Estimating soil parameters important for lifeline siting using system identification techniques.* NISTIR 5145. p. 91. Gaithersburg, MD:NIST.

Holzer, T. L., Youd, T. L., & Bennett, M. J. (1989). In situ measurement of pore pressure build-up during liquefaction. N. J. Raufaste, *Proceedings of the 20th joint panel meeting of the U.S.-Japan cooperative program in wind and seismic effects. 24* Gaithersburg, MD. (NIST SP 760) 118-130.

Hudnut, K. W., & Sieh, K. E. (1989). Behavior of the Superstition Hills fault during the past 330 years. *Bulletin of the Seismological Society of America,* 79(2), 309-329.

Hushmand, B., Scott, R. F., & Crouse, C. B (1992). In-place calibration of USGS pore pressure transducers at Wildlife Liquefaction Site, California, USA., *Proceedings of the Tenth World Conference on Earthquake Engineering. 3* Madrid. 1263-1268. Rotterdam: Balkema.

Hushmand, B., Scott, R. F., & Crouse, C. B. (1991). In-situ calibration of USGS piezometer installations. *Recent advances in instrumentation, data acquisition and testing in soil dynamics.* G.S.P. 29, Orlando, FL. 49-69. ASCE: New York.

Hwang, L. J., Magistrale, H , & Kanamori, H. (1990). Teleseismic source parameters and rupture characteristics of the 24 November 1987, Superstition Hills earthquake *Bulletin of the Seismological Society of America,* 80(1), 43-56.

Johansson, R. (1993). *System identification and modeling* p.512. Englewood Cliffs, NJ: Prentice-Hall.

Kalman, R. E. (1960). A new approach to linear filtering and prediction problems. *Transactions of the ASME, journal of basic engineering,* (3), 35-45.

Ljung, L. (1987). *System identification: theory for the user.* Englewood Cliffs, NJ: Prentice-Hall.

Ljung, L. (1979). Asymptotic behavior of the extended Kalman filter as a parameter estimator for linear systems. *IEEE transactions on automatic control, AC-24*(1), 36-50.

Magistrale, H., Jones, L., & Kanamori, H. (1989) The Superstition Hills, California earthquakes of 24 November 1987). *Bulletin of the Seismological Society of America*, 79(2), 239-251.
MathWorks, (1991). *System identification toolbox*, (Ljung, L. J.). Natick, MA: The MathWorks Inc.
Nazarian, S., & Stokoe II, K. H. (1984). In situ shear wave velocities from spectral analysis of surface waves. *Proceedings, eighth world conference on earthquake engineering. III* San Francisco, CA. 31-38. Englewood Cliffs: Prentice-Hall.
Pandit, S. M., (1991). *Modal and spectrum analysis: data dependent systems in state space*. p. 415. New York: Wiley.
Robinson, E. A. (1982). A historical perspective of spectrum estimation. *Proceedings of the IEEE, 70*(9), 885-907.
Safak, E. (1988). *Analysis of recordings in structural engineering: adaptive filtering, prediction, and control.* (Open-File Report 88-647). Menlo Park, CA: U.S. Geological Survey.
Scott, R. F. (1986). Solidification and consolidation of a liquefied sand column. *Soils & foundations, 26*(4), 23-31.
Sorenson, H. W. (1970). Least-squares estimation: from Gauss to Kalman. *IEEE spectrum*, 7(7), 63-68.
Wald, D. J., Helmberger, D. V., & Hartzell, S. H. (1990). Rupture process of the 1987 Superstition Hills earthquake from the inversion of strong-motion data. *Bulletin of the Seismological Society of America*, 80(5), 1079-1098.

TABLES

Table 1 Summary of system parameters estimated for pertinent times during the Superstition-Hills earthquake.

	1st Mode			2nd Mode			3rd Mode		
Time (s)	f (Hz)	ζ (%) crit.	p	f (Hz)	ζ (%) crit.	p	f (Hz)	ζ (%) crit.	p
*-4·2.8**	*3.7*	*4*	*0.82*	*6.2*	*16*	*-0.03*	*11*	*14*	*-2.5*
*2 8:8.8**	*2.4*	*87*	0.26	3.5	*15*	*0.95*	9.2	*7*	*-0.72*
26♣	0.8	5	0.19	5.3	22	0.26	10.1	*9*	0.43
32♣	0.42	27	0.13	5.3	27	0.24	10.1	*13*	0.31
37♣	0.35	34	0.10	5.3	28	0.24	10.1	*14*	0.30
56♣	0 35	20	-0.02	5.8	44	-0.20	10.0	*23*	0.22
72♣	0.21	45	0.08	7.1	66	0.50	9 8	*31*	0.41

f = resonant frequency; ζ = critical damping; P = participation factor.

NOTE – * indicates ARX (stationary) estimate using combined model; ß indicates instantaneous Kalman (recursive) estimate (i.e., the best values for the point in time shown).

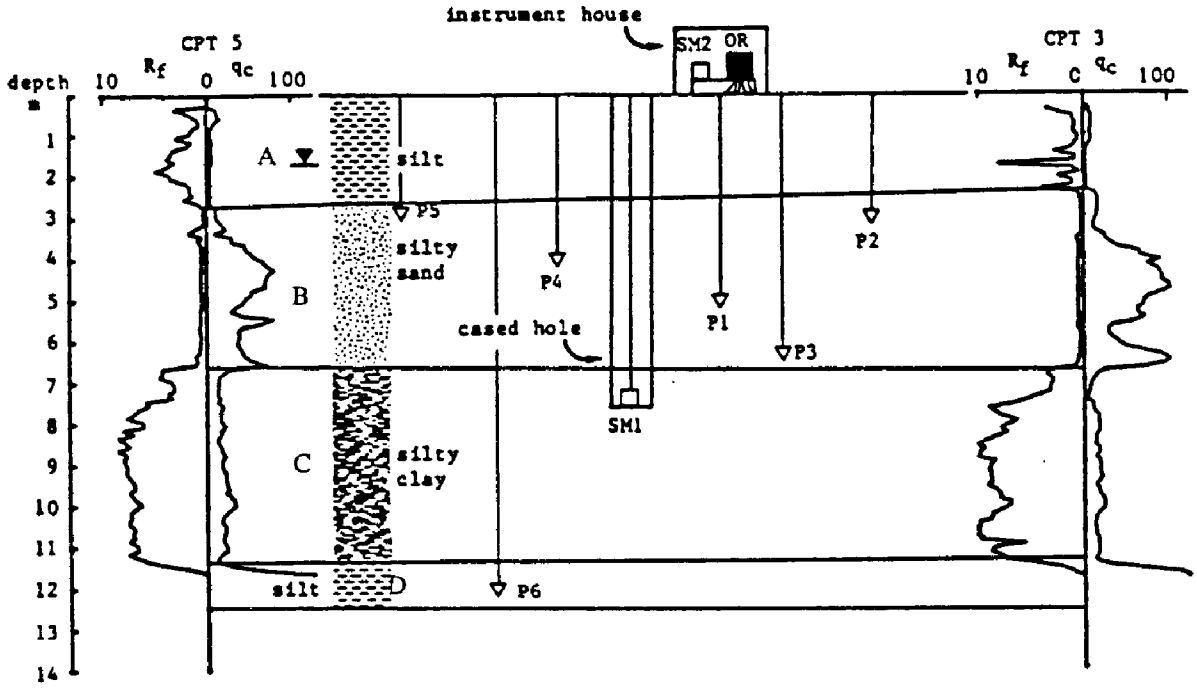

Fig. 1 Layout of the instrumentation at the Wildlife Site (Bennett et al., 1984).

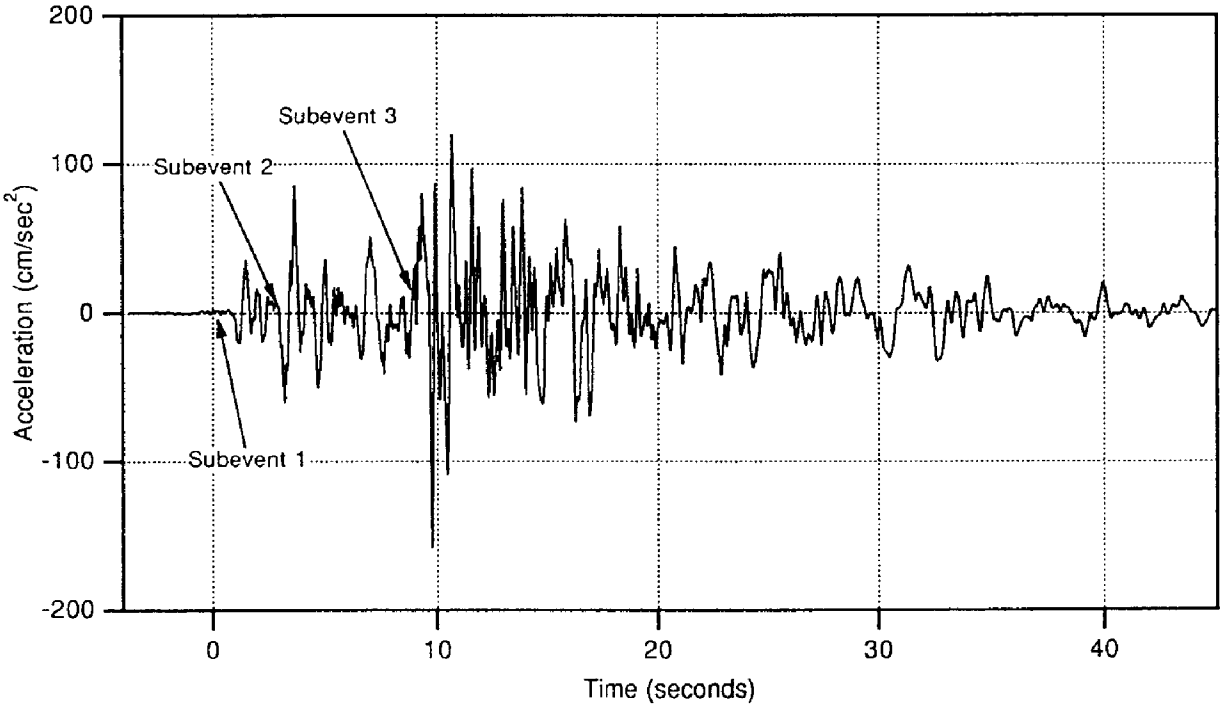

Fig. 2 Acceleration record at a depth of 8 m, N-S direction, Superstition Hills earthquake.

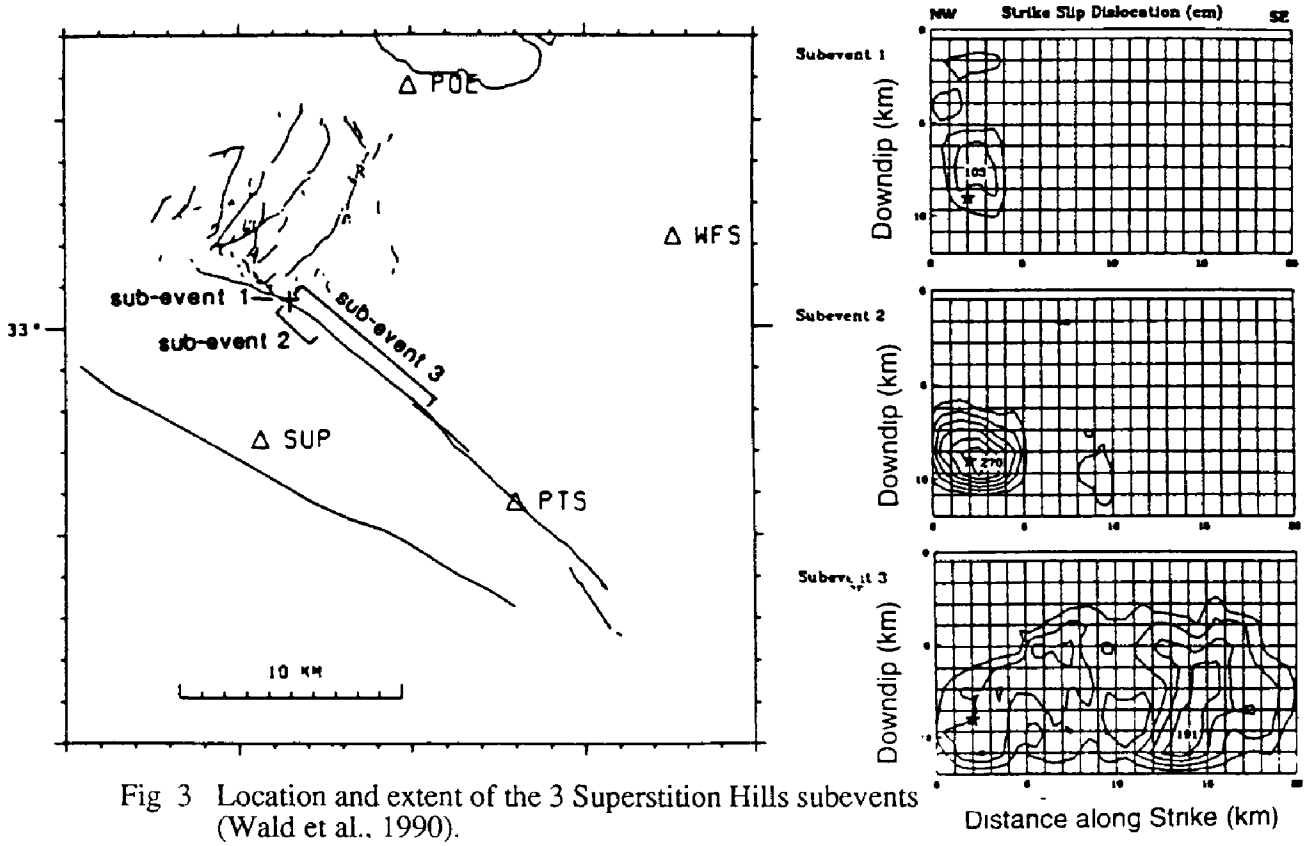

Fig 3 Location and extent of the 3 Superstition Hills subevents (Wald et al., 1990).

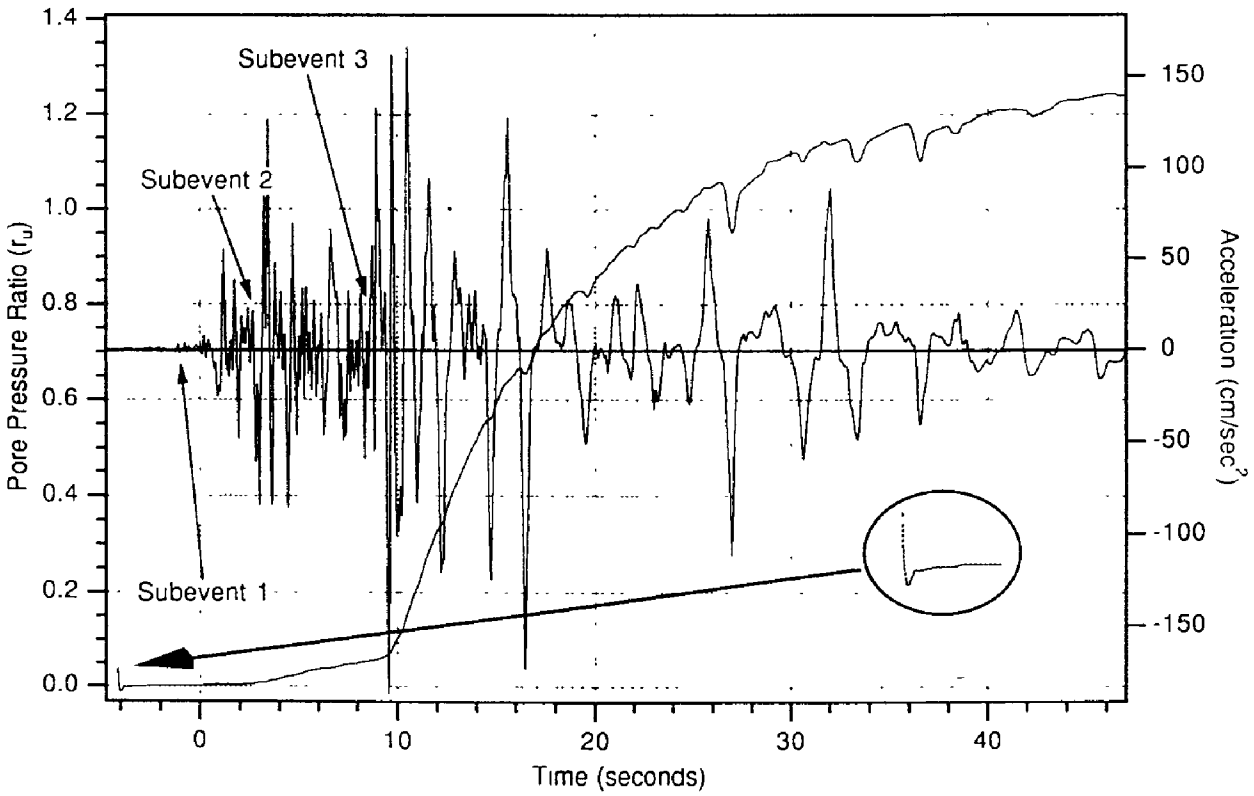

Fig. 4 Pore pressure ratio history compared to top N-S acceleration. Note warm-up detail in inset.

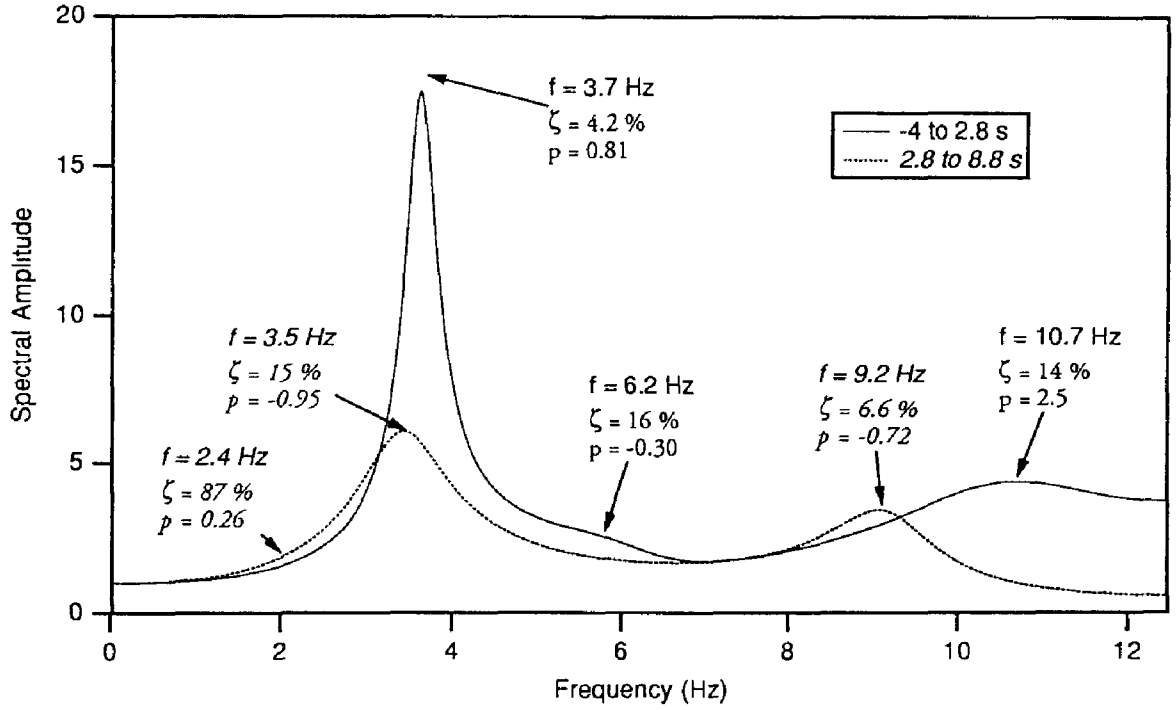

Fig. 5 Spectral estimates for the first and second segments, with estimates of natural frequency, damping ratio, and participation factor.

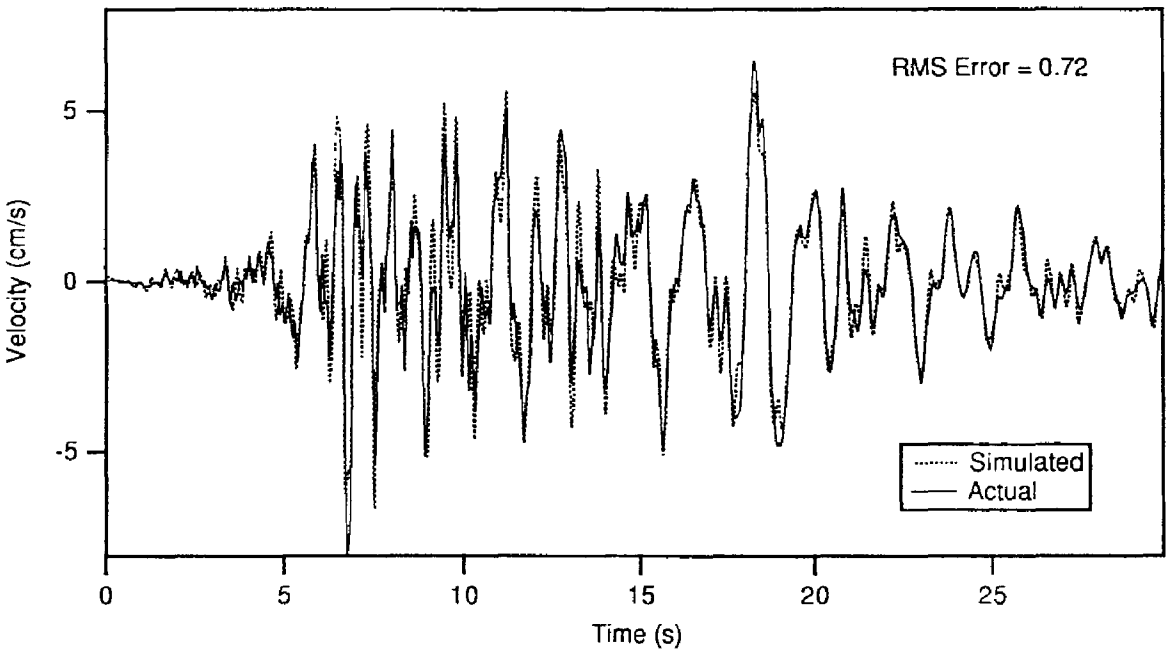

Fig. 6 Comparison between the Elmore Ranch velocity history simulated by the second segment Superstition Hills filter, and the actual velocity history.